Self-Assembly of Mesoscale Objects into Ordered Two-Dimensional Arrays

Ned Bowden, Andreas Terfort, Jeff Carbeck,
George M. Whitesides*

Regular arrays of topologically complex, millimeter-scale objects were prepared by self-assembly, with the shapes of the assembling objects and the wettability of their surfaces determining the structure of the arrays. The system was composed of solid objects floating at the interface between perfluorodecalin and water and interacting by lateral capillary forces; patterning of the wettability of the surfaces of the objects directs these forces. Self-assembly results from minimization of the interfacial free energy of the liquid-liquid interface. Calculations suggest that this strategy for self-assembly can be applied to objects on a micrometer scale.

This report describes the directed self-assembly of small objects (between 1 and 10 mm in length) into regular, two-dimensional arrays. It extends ideas emerging from molecular self-assembly to much larger objects and describes an approach for the fabrication of complex systems that has potential for application in microelectronics, optics, microelectromechanical systems, and displays (*1*). These self-assembled systems have analogies to bubble rafts (*2*, *3*) and related aggregates formed by spheres on surfaces (*4*, *5*); they differ in that the use of nonspherical objects with designed shapes and wettabilities makes it possible to generate aggregates with complex structures.

The individual objects were made of polydimethylsiloxane (PDMS), a hydrophobic polymer with a surface free energy (γ_{SV}) equal to 22 to 24 erg cm^{-2} (*6*–*8*). First, the PDMS was cured in a mold of the desired shape. Designated surfaces were then made hydrophilic by oxidation with an O_2 plasma (*6*, *9*); surfaces that were to be hydrophobic were either covered with tape before the oxidation or generated by cutting of the PDMS after oxidation to expose a fresh hydrophobic surface. For each of the objects in Fig. 1, the lower face [the face in contact with the perfluorodecalin ($C_{10}F_{18}$)] was hydrophobic, and the sides were either hydrophobic or hydrophilic according to the design summarized in the insets. The upper face was usually made hydrophilic to prevent any $C_{10}F_{18}$ from settling on top of the objects and causing them to sink into the $C_{10}F_{18}$-H_2O interface. The $C_{10}F_{18}$ wetted the hydrophobic sides and formed menisci; the hydrophilic sides barely perturbed the $C_{10}F_{18}$-H_2O interface (*10*, *11*). The system was placed on a rotary shaker that oscillated gently in the plane of the interface. The frequency of rotation was adjusted for each system to allow the in-plane movement of the liquid to bring the objects close to one another and to break up misformed aggregates; a typical frequency was 1 to 2 Hz. When two hydrophobic sides of PDMS came within a critical distance of one another (~5 mm), they moved into contact. This movement was driven by the minimization of the interfacial free energy of the system, caused by eliminating the curved menisci at the hydrophobic surfaces. A thin layer of $C_{10}F_{18}$ remained between the objects, even at their closest contact (*12*). Self-assembly was completed after ~5 to 30 min.

A variety of self-assembled arrays can be made by controlling the hydrophobicity of the sides of the objects (Fig. 1A). The contrast between Fig. 1B and Fig. 1C demonstrates the level of control that we can achieve: In Fig. 1B, alternate sides of the hexagons are hydrophobic and the objects form an open network; in Fig. 1C, all of the sides of the hexagons are hydrophobic and the objects form a close-packed array.

A shape-selective lock-and-key geometry allows the formation of aggregates from more than one component (Fig. 2, A through C). The objects in Fig. 2A have three favorable choices for contact (Fig. 2C). The amplitude of oscillation of the system during equilibration was set to be large enough to break apart pairs interacting head-to-head and tail-to-tail but to leave together those interacting more strongly head-to-tail. Head-to-tail contact is favored energetically by two complementary factors: it maximizes the area of hydrophobic surface in close proximity; and it is kinetically stable to dissociation caused by stirring, because the oscillating motion at the interface—a motion that seems to in-

Department of Chemistry and Chemical Biology, Harvard University, 12 Oxford Street, Cambridge, MA 02138, USA.

*To whom correspondence should be addressed.

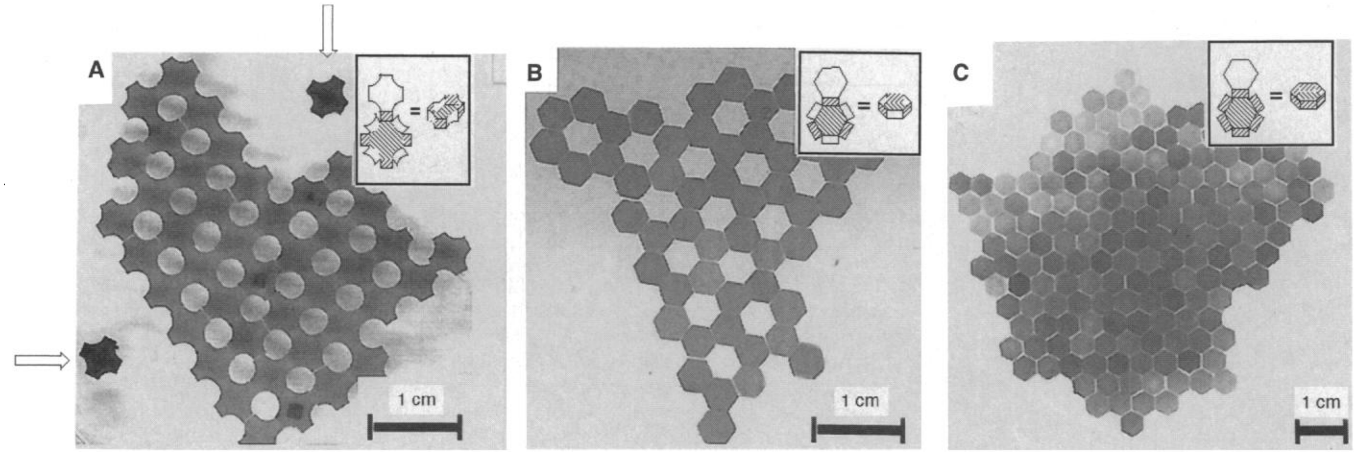

Fig. 1. Crystalline aggregates generated by the self-assembly of (**A**) crosses, (**B**) hexagons in an open network, and (**C**) hexagons close-packed. Panel (A) shows an extended two-dimensional square array formed from crosses having hydrophobic ends; the two crosses with arrows pointed toward them were completely oxidized; these pieces were rejected by the array. They clearly show the shape of the individual pieces. Hatched faces in the insets indicate hydrophobic surfaces and white faces indicate hydrophilic surfaces. The top faces are clear and hydrophilic.

fluence the objects primarily by shear—has minimal influence on pairs of objects once assembled into a head-to-tail configuration.

A third method for self-assembly uses the area of hydrophobic side surfaces, and thus the strength of the attractive capillary force, to direct the self-assembly of different objects (Fig. 3, A through D). A mixture of two types of PDMS objects with the same square bases, but heights that differed by a factor of 5, were agitated at the interface between $C_{10}F_{18}$ and water. The order of the attractive forces in the system was tall-tall > tall-short > short-short. The degree of agitation was set to allow the tall objects to form an array; when agitation was stopped, the short objects coagulated around this array in a disordered state.

The above experiments were carried out with objects having dimensions of 1 to 10 mm. We investigated the lower limits to the size of the objects that could be assembled by lateral capillary forces at the $C_{10}F_{18}$-H_2O interface by calculating the change in interfacial free energy as two perpendicular surfaces moved from infinite separation to some finite separation, d. We calculated the height h (in meters) of the $C_{10}F_{18}$-H_2O interface between the two objects using the linearized Laplace equation (*13*) (Fig. 4A)

$$\frac{\partial^2 h}{\partial x^2} = \frac{1}{\gamma}(\Delta\rho g h - \Delta P_0) \qquad (1)$$

where γ (in joules per square meter) is the interfacial free energy, $\Delta\rho$ (in kilograms per cubic meter) is the difference in density between the two fluids, the zero for h is set at the $C_{10}F_{18}$-H_2O interface far from the objects, g (in meters per second per second) is the acceleration due to gravity, and ΔP_0 (in pascals) is the change in pressure across the interface at $x = 0$. If we assign a value of $h(0) = 0$, then the value of ΔP_0 does not enter into the solution of Eq. 1. Using the boundary conditions $h(r) = t$, where t (in meters) is the thickness of the object and $(\partial h/\partial x)_{x=0} = 0$, we find that the solution of Eq. 1 is

$$h(x) = t\left[\frac{2}{1 - e^{(d/x_c)}} + \frac{e^{(-x/x_c)} + e^{(x/x_c)}}{e^{(d/2x_c)} - e^{(-d/2x_c)}}\right] \qquad (2)$$

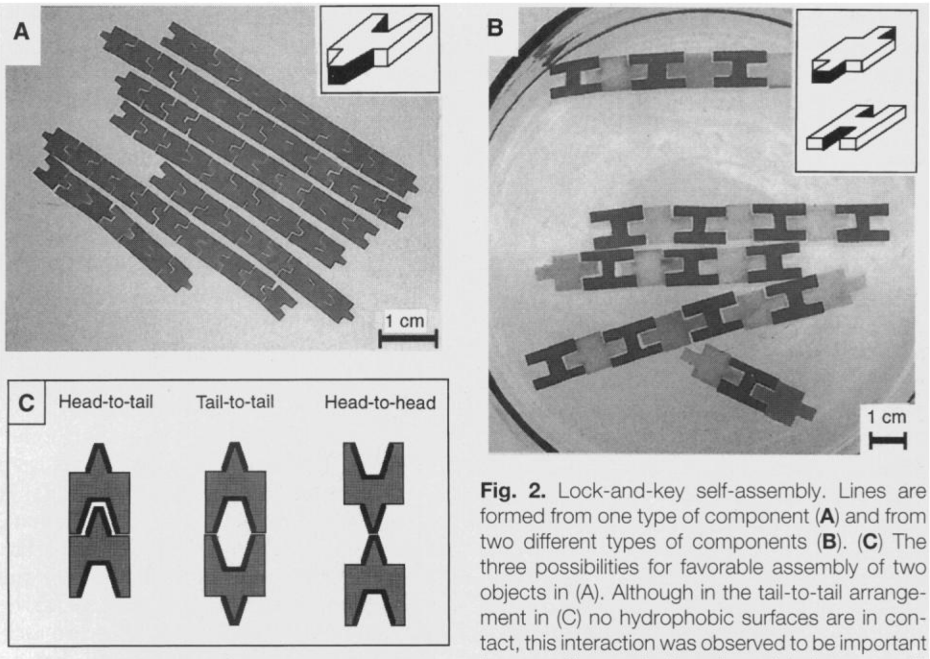

Fig. 2. Lock-and-key self-assembly. Lines are formed from one type of component (**A**) and from two different types of components (**B**). (**C**) The three possibilities for favorable assembly of two objects in (A). Although in the tail-to-tail arrangement in (C) no hydrophobic surfaces are in contact, this interaction was observed to be important because the menisci are brought close enough together to interact. Dark faces in the insets in (A) and (B) indicate hydrophobic sides and white faces indicate hydrophilic sides. The top faces are clear and hydrophilic.

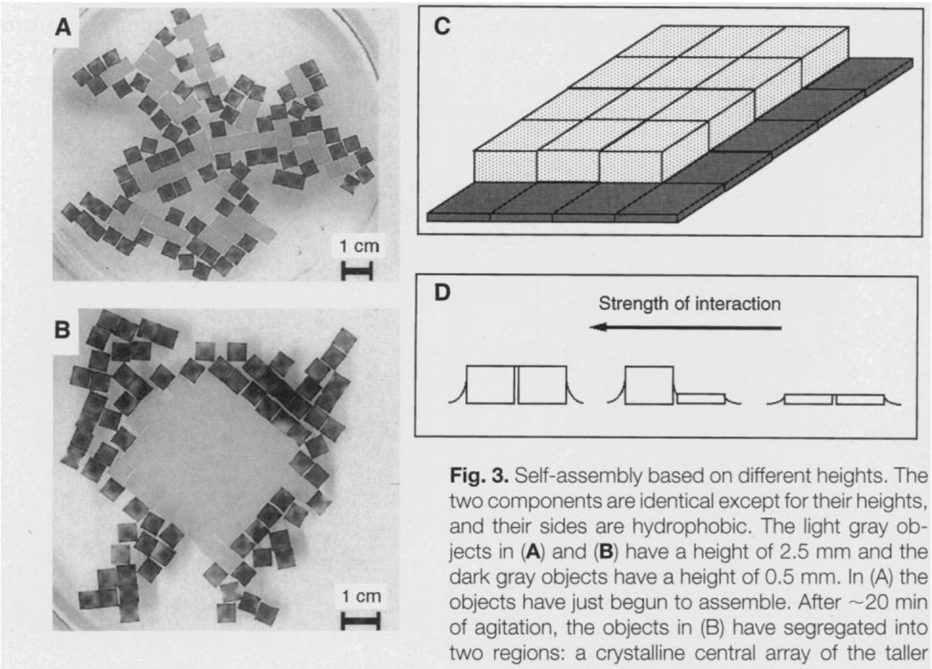

Fig. 3. Self-assembly based on different heights. The two components are identical except for their heights, and their sides are hydrophobic. The light gray objects in (**A**) and (**B**) have a height of 2.5 mm and the dark gray objects have a height of 0.5 mm. In (A) the objects have just begun to assemble. After ~20 min of agitation, the objects in (B) have segregated into two regions: a crystalline central array of the taller objects, surrounded by a disordered collection of the smaller ones. (**C**) A schematic view of the interaction of the objects of different heights. (**D**) Side view of the three different interactions when two pieces of PDMS with different heights are assembled. The strength of interaction increases from right to left.

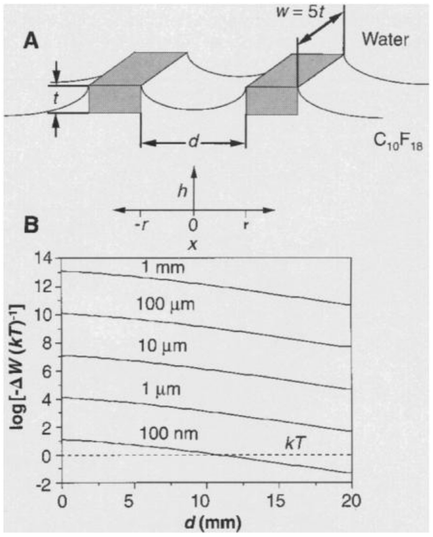

Fig. 4. (**A**) The coordinate system for Eqs. 1 and 2. The objects have a height of t and a width of $w = 5t$, and their proximate surfaces are separated by d. (**B**) The logarithm of the change in interfacial free energy—divided by thermal energy, kT—in bringing two surfaces from infinite separation to a finite separation, d, is plotted for heights from t = 1 mm to 100 nm.

where we have made the replacement $x_c = (\gamma/\Delta\rho g)^{1/2}$. For infinite d the capillary surface is given by a simple exponential decay with $h(x) \propto e^{(-x/x_c)}$.

To estimate the change in interfacial energy as a function of distance, we calculated the difference in the arc length $\Delta\ell$ (in meters), defined by $h(x)$ for two surfaces separated by d and two surfaces separated by an infinite distance; the change in arc length was then multiplied by the width of the object w (in meters), and the interfacial free energy to yield the change in interfacial free energy (*14*). As a model system, we assigned a length to the perpendicular surface equal to five times the height. This model gave a change in interfacial free energy, ΔW, of $\Delta W = 5\Delta\ell\gamma t$. From the change in interfacial free energy for heights from t = 1 mm to 100 nm (Fig. 4B), we conclude that the energetics for self-assembly are favorable for objects with t as small as 100 nm. For the two-dimensional self-assembly of spheres, the radius at which $\Delta W/kT \sim 1$ (where kT is the thermal energy) has been calculated to be on the order of 1 to 10 μm (*15*, *16*). Self-assembly driven by capillary forces between conformal surfaces should therefore make possible the assembly of much smaller objects than would be possible with spheres; the ability to control the shapes and interfacial properties of these objects makes it possible to design the geometries of the resulting arrays.

Four factors contribute to the success of this strategy for the directed self-assembly of small objects. First, the aggregates are energetically more stable than the individual dissociated objects or disordered aggregates. Second, formation of the aggregates is reversible when the system is agitated: formation and dissociation of the aggregates compete. The aggregates are therefore able to reach the energetically most stable form. Third, the hydrophobic sides are attracted to one another over large distances (about two to three times the dimension of the height), leading to relatively rapid assembly. Fourth, even when two hydrophobic sides are in close proximity, they can move laterally from side to side, lubricated by the intervening film of $C_{10}F_{18}$, and can thus maximize the amount of hydrophobic area in contact.

REFERENCES AND NOTES

1. There are few methods for assembling arrays of small objects. See (*2*, *4*, *5*); J. K. Tu, J. J. Talghader, M. A. Hadley, J. S. Smith, *Electron. Lett.* **31**, 1448 (1995); A. Ashkin and J. M. Dziedzic, *Science* **235**, 1517 (1987); K. Svoboda and S. M. Block, *Annu. Rev. Biophys. Biomol. Struct.* **23**, 247 (1994).
2. A. W. Simpson and P. H. Hodkinson, *Nature* **237**, 320 (1972).
3. S. T. Schober, J. Friedrich, A. Altmann, *J. Appl. Phys.* **71**, 2206 (1992).
4. M. Yamaki, J. Higo, K. Nagayama, *Langmuir* **11**, 2975 (1995).
5. P. A. Kralchevsky and K. Nagayama, *ibid.* **10**, 23 (1994).
6. PDMS is easy to fabricate and its solid-liquid interfacial free energy can be readily controlled by oxidation to make the surfaces hydrophilic or hydrophobic. We placed the PDMS structure into a plasma cleaner for 5 min under O_2 at a pressure of 0.20 torr to oxidize the PDMS. The oxidation of PDMS is believed to result in a surface that comprises SiOH groups. The contact angle of water on oxidized PDMS is less than 15°.
7. M. J. Owen, *J. Coatings Technol.* **53**, 49 (1981).
8. W. A. Zisman, in *Symposium on Adhesion and Cohesion*, P. Weiss, Ed. (Elsevier, New York, 1962), p. 176.
9. D. W. Fakes, M. C. Davies, A. Browns, J. M. Newton, *Surf. Interface Anal.* **13**, 233 (1988).
10. The perfluorodecalin wet the unoxidized PDMS and formed a meniscus; the water wet the higher energy surface of oxidized PDMS. The capillary forces acting at the oxidized surfaces were very weakly attractive compared to those of the hydrophobic surfaces, because the PDMS (density = 1.05 g ml^{-1}) does not sink far enough into the perfluorodecalin (density = 1.91 g ml^{-1}) to generate a meniscus with significant curvature at the hydrophilic interfaces. Other fluorinated alkanes with properties similar to those of perfluorodecalin were used with equal success.
11. C. D. Dashkin, P. A. Kralchevsky, W. N. Paunov, H. Yoshimura, K. Nagayama, *Langmuir* **12**, 641 (1996).
12. The evidence that a thin layer of $C_{10}F_{18}$ remained between the PDMS solids at their closest contact is indirect: When two flat pieces of PDMS come in contact in water with no $C_{10}F_{18}$ present, they stick to each other strongly, and this process is effectively irreversible. If we add $C_{10}F_{18}$ to the water after the PDMS solids have come into contact, they remain stuck to one another.
13. H. T. Davis, *Statistical Mechanics of Phases, Interfaces and Thin Films: Advances in Interfacial Engineering* (VCH, New York, 1996).
14. In performing these calculations, we used values of γ = 0.05 J m^{-2} and $\Delta\rho$ = 900 kg m^{-3} for the $C_{10}F_{18}$-H_2O interface.
15. P. A. Kralchevsky, V. N. Paunov, N. D. Denkov, I. B. Ivanov, K. Nagayama, *J. Colloid Interface Sci.* **155**, 420 (1993).
16. V. N. Paunov, P. A. Kralchevsky, N. D. Denkov, K. Nagayama, *ibid.* **157**, 100 (1993).
17. We thank M. Mammen for helpful comments and suggestions. Funded by NSF grant CHE-9122331, the Office of Naval Research, and the Defense Advanced Research Projects Agency. N.B. was supported by a predoctoral fellowship from the Department of Defense. A.T. thanks the Deutsche Forschungsgemeinschaft for a research grant.

4 November 1996; accepted 24 February 1997

Permo-Triassic Boundary Superanoxia and Stratified Superocean: Records from Lost Deep Sea

Yukio Isozaki

Pelagic cherts of Japan and British Columbia, Canada, recorded a long-term and worldwide deep-sea anoxic (oxygen-depleted) event across the Permo-Triassic (or Paleozoic and Mesozoic) boundary (251 ± 2 million years ago). The symmetry in lithostratigraphy and redox condition of the boundary sections suggest that the superocean Panthalassa became totally stratified for nearly 20 million years across the boundary. The timing of onset, climax, and termination of the oceanic stratification correspond to global biotic events including the end-Guadalupian decline, the end-Permian extinction, and mid-Triassic recovery.

The greatest mass extinction in the Phanerozoic occurred at the timing of the Permo-Triassic (P-T) boundary; many hypotheses for the extinction have focused on changes in the ocean, including development of overturn of an anoxic ocean (*1*, *2*). One problem has been that most records of the boundary are in shallow-water sedimentary rocks that formed around the supercontinent Pangea. Recently, however, P-T boundary sections were discovered in deep-sea cherts that crop out extensively in the Jurassic accretionary complex in southwest Japan (*3*, *4*). The cherts represent ancient pelagic sediments primarily deposited in a mid-oceanic deep sea of the superocean Panthalassa and accreted onto the South China (Yangtze) continental margin in the Middle Jurassic (*5*). The Panthalassa superocean occupied nearly 70% of Earth's surface in the Late Permian (*6*). Rocks near the P-T boundary are reduced, and are thought to have been deposited in an anoxic environment (*3*, *4*, *7*, *8*). I refer to these rocks as the P-T boundary unit (PTBU; Fig. 1). Across the PTBU, Paleozoic radiolarians (planktonic protozoans) are completely replaced by distinct Mesozoic types. Similar rocks have also recently been found in British Columbia, Canada. I used the sections from Japan and British Columbia to evaluate Panthalassa ocean dynamics across the P-T boundary.

In the Japanese sections, Early to early Late Permian and Middle to Late Triassic cherts are composed mainly of siliceous radiolarian tests (~95% by weight) and are mostly brick red in color. X-ray diffraction and ^{57}Fe Mössbauer spectroscopy demon-

---

Department of Earth and Planetary Sciences, Tokyo Institute of Technology, O-okayama, Meguro, Tokyo 152, Japan. E-mail: yisozaki@geo.titech.ac.jp